NASA CR 11198
October 1971

Turbulent Jet Mixing in a Supersonic Stream

R. C. Swanson and J. A. Schetz
Department of Aerospace Engineering

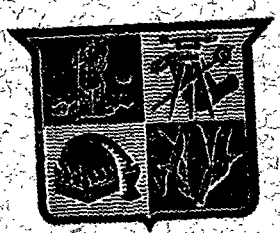

College of Engineering,
Virginia Polytechnic Institute
and State University

NASA CR-111981

TURBULENT JET MIXING IN A SUPERSONIC STREAM

By R. C. Swanson and J. A. Schetz

Prepared Under Contract No. NAS1-10233
Aerospace Engineering Department
Virginia Polytechnic Institute and State University
Blacksburg, Virginia 24061

for

NATIONAL AERONAUTICS AND SPACE ADMINISTRATION

SUMMARY

An experimental study of turbulent, subsonic, co-axial jet mixing of air in a supersonic air stream is presented. The nominal test conditions for the experiments performed are as follows: $M_\infty \approx 3.5$, $P_o = 134$ psia, $T_o = 540°$. Data taken at five axial stations downstream of the exit of the jet supply tube, which was suspended through the nozzle throat of a supersonic wind tunnel, are given in the form of total pressure, Mach number, and velocity distributions. There is also included an investigation of the effect of swirl as a mixing aid. Swirl, produced by tangential injection of 50% of the total air mass flow leaving the jet supply tube, is examined through Schlieren photographs and total pressure surveys. From a comparison of non-swirl and swirl data, it is concluded that the swirl has no discernible effect on the mixing.

TABLE OF CONTENTS

LIST OF FIGURES

NOMENCLATURE

D = O.D. of jet supply tube

L = length of swirl tube (for injection)

M = Mach number

P = pressure

R = gas constant (air)

S = swirl number

T = temperature

U = velocity

X = distance down stream of jet exit

$\dot{m}$ = mass flow rate

r = radius

γ = ratio of specific heats (C_p/C_v)

ρ = density

Subscripts

A = axial flow

C = center line condition

S = peripherial flow

c = condition on cone surface

e = edge of mixing region

i = inner radius (center of jet supply tube to swirl tube)

o = tunnel stagnation condition

t_1 = stagnation condition in front of normal shock

t_2 = stagnation condition behind normal shock

o' = inner radius of supply tube

∞ = free stream

INTRODUCTION

In recent years co-axial jet mixing problems have received considerable attention due to the many practical situations in which they are encountered. Moreover, a large amount of material has been published concerning such problems, e.g. Ref. (1). Since all turbulent shear flow "theories" are based upon empirical information, there has been substantial emphasis on experimental work. In Ref. (2), the existing experiments with a jet in a co-flowing stream are listed and summarized. An examination of this tabulation reveals little detailed data for the case where the external stream is highly supersonic; in fact, most of the data is limited to quite low Mach numbers ($M \leq 1.5$). However, such practical considerations as supersonic combustion chambers and jet ejectors require investigation of turbulent, co-axial jet mixing in a strongly supersonic stream.

Another important aspect of mixing problems concerns mixing aids. Many practical devices use swirl as a mixing aid. For example, in low speed combustion chambers swirling jets are used to control the heat release zone and the rate of burning. Since swirl is an easy device to employ, it may be of interest in other applications such as supersonic combustion. At this point there have been no studies of initial swirl in the injectant when the external stream is supersonic. Previous work, confined primarily to jets in a quiescent or subsonic medium, provide some pertinent quantitative and qualitative information, i.e. Refs. (4) and (5). In these studies a non-dimensional quantity called the "swirl number" is used to define the

degree of swirl. This number is given by the ratio of axial flux of angular momentum to the product of axial flux of linear momentum and a characteristic radius. Test results indicate an increase in mixing with an increase in swirl number. On the basis of such considerations, an experimental investigation of supersonic jet mixing, with and without swirl, has been undertaken.

In the first section of this report, a complete description of the equipment and test methods employed in the research is given. The techniques applied in data reduction are also included. Then, the experimental results are presented and discussed.

APPARATUS AND TEST METHODS

A. Wind Tunnel Facilities

Tests were conducted in the 9" x 9" supersonic wind tunnel in the Gas Dynamics Lab at V.P.I.&S.U. This facility is of an intermittent, blow-down type with interchangeable contoured nozzles. A complete description of the tunnel is given in Appendix B. The Mach 4.016 nozzle was used for this experimental effort. The average starting tunnel total pressure and total temperature were 145 psia and 546°R, respectively. During the tests there was a slow linear decrease in both total pressure and total temperature. There were also some small deviations from this trend. In order to account for these variations, all recorded pressures and temperatures were non-dimensionalized by their corresponding stagnation conditions at the time the measurements were taken. Test runs were approximately 12 seconds in duration.

B. Injection Model

The basic part of the test apparatus was a stainless steel tube 38 inches long with an O.D. of .375 inches and an I.D. of .350 inches. This tube was suspended through the nozzle throat in the manner indicated in Figures 1 and 2. Vibration due to the length of the tube and the severe starting and stopping loads of the tunnel necessitated additional support of the jet supply tube. In order to minimize distortion of the mixing field, support wires rather than struts were used to prevent tube movement. There were two sets of four stainless steel wires, each with a diameter of

.025 inches. The leading set and the rear set were located at 5.25 inches and 19.2 inches behind the jet exit, respectively. Since it was desirable to be able to replace broken wires with the minimum of difficulty, the jet supply tube was soldered to a conical piece that screwed into the supply chamber, as shown in Figure 2. This meant that an arrangement was needed so that the wires could be returned to the correct orientation after the tube had been rotated. First, the supply tube was cut at the two positions where the wires were to be located. Then, as illustrated in Figure 3, the integrity of the tube was restored with inner stainless steel tubes surrounded by two stainless steel sleeves, .563 inches long. All connections were soldered except the sleeve to which the wires were to be attached; this could be rotated. The ends of the support wires, set in shallow grooves in the sleeves, were soldered just enough to keep them in place. To insure a secure attachment, .025 inch tinned copper wire was wrapped around the wires and soldered for a length of .5 inches along the sleeves. When the sleeves were correctly oriented, the grooves made an angle of 60° with respect to the vertical plane. The front wires extending from the jet supply tube were connected to turn-buckles located above and below the front of the nozzle block. Figure 1a shows both these and the rear ones, which were connected to turn-buckles located on the side of the nozzle section. The wires were equi-tensioned so as to keep the jet tube in the center of the test section during the tests. With respect to the tube, the angle of inclination of the front wires was approximately 33° while that of the back wires was approximately 56°. The average life time of the support wires before failure due to

fatigue was found to be roughly 75 tests.

Another important part of the injection system was the swirl tube. In order to produce swirl, air was injected tangentially inside the main jet supply tube. The swirl production device was a .050 O.D. by .033 I.D. stainless steel tube crimped on the end and soldered to the inside of the main tube .875 inches from the exit (Figure 3). At .1875 inches from the end of the swirl tube, there were five holes with a diameter of .018 inches spaced .125 inches apart drilled into the side. Air exiting from these holes was therefore directed around the periphery of the main jet flow. There were separate air sources for the swirl tube and the axial flow tube.

The air source for the tunnel was also used to supply air for the main jet. Bottled air was the source for the swirl injection system. For both cases the mass flow was measured with Fisher Rotameter flow meters. Conversion formulas and corresponding sample calculations to determine flow settings at the desired test conditions are given in Appendix C. The capacity of the flow meter for the jet, designated FM1, was 4.87 scfm at an operating pressure of 19.4 psig and temperature of 70°F. To prevent a shock in the jet, a mass flow of 1.37 scfm was used. This number was obtained by picking a mass flow too high and continuously reducing same until no shock structure appeared in the jet. After leaving FM1, the air entered the test apparatus by way of two .375 inch copper tubing connections. The air then entered the 1.5 inch O.D. by .25 inch wall chamber through four .25 inch stainless steel tubes (Figure 1b). The capacity of the flow meter for the air injected tangentially, designated FM2, was 1.15 scfm at an operating pressure of

140 psig and temperature of 70°F. Once the bottled air left FM2, it went directly into the swirl tube. For the tests conducted with swirl, an air mass flow of .685 scfm was used for both the axial flow and the peripheral injection.

C. Pressure Measurements

Pressure distributions were obtained to define the flow field. With the pressure rake shown in Figure 4, pitot pressure surveys were taken at five axial stations, X/D = 5, 10, 15, 20, 25. The pitot tubes were assigned numbers for identification as indicated in Figure 4. The distances between the pitot tubes are listed in Table D-8. Vertical ports 8 and 5 and lateral ports 9 and 10 were located symmetrically about port 7 so that the rake could be centered in the jet by matching pressures. The details of the centering process are discussed in the experimental procedure. Another feature of the rake was the 10° half angle brass cone static probe (Figure 5). The base of the cone was .062 inches, and the tip was precision ground to a sharp point. At .1094 inches from the tip of the cone, there were four .013 inch ports drilled perpendicular to the surface and 90° apart. The recorded pressure was the average of these four ports. This probe was located at the mirror image of port 0, so that the Mach number variations could be determined easily if the static pressure change across the mixing region were small.

Two key devices were used in positioning the rake for taking the surveys. A steel strut with a 14° wedge leading edge was used to hold the rake (Figure 1c). The strut was 20.5 inches high with a base 6 inches by 3 inches by .5 inches. There was a .625 inch diameter hole 20 inches

above the base for the rake. The base of the strut was bolted to a milling machine bed. This device, displayed in Figure 1c, was used for both lateral and vertical positioning of the rake. The micrometer associated with vertical location of the rake was graduated in .001 of an inch. The micrometer that indicated lateral position was marked in .0005 of an inch. Thus, there was sufficient fine adjustment for centering the rake.

The pressure leads from the rake, including the static pressure lead, were connected to a Model 48J9-1021 Scani-valve. Since this Scani-valve has 48 ports, the pressure field could be scanned twice per test or nearly so as determined by scan rate and tunnel run time. A time step of .5 seconds was chosen so that the static pressure could also be read from the Scani-valve. Another advantage of this device is that it requires only one transducer. In these experiments a Statham ±15 psig transducer was found to be adequate. All pressures were read out on Hewlett Packard strip chart recorders. These are high speed, two-channel potentiometric recorders with a maximum deflection of 10 inches, accurracy of 0.1% of full scale setting, and response time of 0.25 sec.

D. Temperature Measurements

Both the tunnel and the jet total temperatures were measured with Copper Constantan type thermocouples. Temperature measurements were read out on strip chart recorders which have an electric cold junction and indicate temperature directly in °F. Again, the accuracy of the recorders was ±0.1% of the full scale deflection setting. The total temperature probe, shown in Figure 6, was used to investigate the jet. This probe was made from a design developed by Pratt and Whitney.

Details concerning the sensitivity and recovery factor of the probe are given in Ref. 8. The probe was supported and positioned in the same manner as the pressure rake.

E. Optical Methods

Schlieren photographs were taken in order to optically visualize the flow field. A 12 inch Schlieren apparatus with two parabolic mirrors, each having a focal length of 80 inches, and an air cooled high intensity mercury PEK light source was used. In order to depict the turbulent character of the flow field, spark Schlieren pictures were also taken. The light source was an EG&G 549 Microflash system with a 1 μ sec. flash. Photographs were taken on Polaroid type 57 (ASA 3000) sheet film using a Graphlex camera.

EXPERIMENTAL PROCEDURE

The following steps were required to make the pitot pressure surveys at each of the five axial stations:

1. The rake was placed at the appropriate "X" station.
2. Using a precision scale, port 7 of the rake was located on the center line of the test section.
3. A test was then run with no swirl, and the pressures were recorded. The Scani-valve was started as soon as supersonic flow was attained. During the test, a marker was triggered on all recorders simultaneously so that the data could be subsequently correlated with respect to time. Schlieren photographs were also taken.
4. After the test the centering of the jet was checked by examining the pressure readings from ports 8, 5, 9, and 10.
5. The next step in the procedure was to adjust the lateral position of the rake so as to have equal readings from ports 9 and 10. Vertical adjustment was also made in order to equalize the pressures at ports 8 and 5. However, emphasis was placed on lateral positioning since we were concerned to have the rake centered side to side such that the closely spaced probes in the vertical direction were sensing a true radial profile.
6. This technique was continued until pressure readings from ports 8, 5, 9, and 10 were in close agreement.
7. Then, tests with swirl, 50% by mass flow, were run. These tests were conducted in the same manner as those without swirl.

8. Once the necessary agreement for jet centering was obtained, the rake was moved down .524 inches so that the cone static probe would be on the center line of the jet. A test was run, and pressure measurements were taken.
9. With the cone static probe still on the center line, the pressure measurements for the no swirl case were taken.
10. The steps listed above were repeated for stations with X/D = 10, 15, 20,25.

When the pressure surveys were completed, the total temperature in the jet was investigated. First, the total temperature probe was positioned on the center line of the jet at the axial station X = 10D. A test was then run, and the total temperatures measured in the tunnel settling chamber and the jet were compared. Each test showed the jet total temperature trace closely following the T_o cooling trace. The maximum temperature difference was 5°R. This result was felt to be sufficient basis for taking the total temperature to be constant throughout the jet; therefore, no additional temperature measurements were taken.

DATA REDUCTION

The initial task in the data reduction was to determine the pressures measured with the rake. Recorded pressures were represented by inches of deflection on strip charts, and these deflections were related to pressure in psig by means of a calibration curve of the transducer used in the Scani-valve. This curve included both the positive and negative ranges of the transducer. A self-regulating precision pneumatic tester (Model 750-B, Mansfield & Green) was used to calibrate the positive range, while a combination of vacuum pump and a Heise pressure gage were used to calibrate the negative range. After obtaining the pitot and cone static pressures at each station, the barometer readings taken before and after each test sequence were averaged, converted to psia, and added to the pressures to convert to psia. The average barometer reading over all test runs was 27.90 in.Hg. Once this was accomplished, all of the pressure measurements were non-dimensionalized by the tunnel total pressure at the time they were recorded. Then, they were corrected to a fixed nominal test tunnel total pressure, i.e. 134 psia. This procedure was followed for both swirl and non-swirl cases.

With the pitot pressure surveys determined, the Mach number distributions at each station were readily deduced. First, the ratio of the cone static pressure to the pitot pressure at port 0 of the rake was found. Second, knowing that this ratio could be expressed as

$$\left(\frac{P_c}{P_\infty}\right)\left(\frac{P_1}{P_{t_1}}\right)\left(\frac{P_{t_1}}{P_{t_2}}\right) \quad , \tag{1}$$

a plot of P_c/P_{t_2} versus M was made. The quantity P_c/P_∞ was obtained from Table 2 of Ref. (6), and Ref. (7) was used to provide the values of the remaining two ratios for different Mach numbers. Next, the Mach number associated with (1) for the particular station in question was determined. Using Ref. (7) again, the quantity P_1/P_{t_2} was found and multiplied by P_{t_2}. Since the static pressure was taken to be constant across the jet, the Mach number distribution was easily derived. That is, each pitot pressure across the jet was divided into the static pressure, and the Mach numbers were found using a graph of P_1/P_{t_2} versus Mach number. With the Mach number variations known, the total pressure and static temperature distributions followed directly.

Ref. (7) provided the ratio P_{t_2}/P_{t_1} for each Mach number. Therefore, the values of P_{t_1} were easily calculated.

Previously, it was stated that experimental evidence supported taking the total temperature constant throughout the jet. The value of the tunnel total temperature used for calculations was 540°R. In order to determine the static temperature variations, the flow was assumed to be adiabatic, the ratios of T/T_t were found in Ref. (7), and each ratio was multiplied by 540°R, the nominal test total temperature. At this point, all the necessary information was available to compute the velocity profiles.

Using the formula

$$U = M\sqrt{\gamma g R T}$$

and the Mach number and static temperature data, the velocity profiles were computed.

As a non-dimensional measure of the degree of swirl, a swirl number was calculated from the following definition:

$$S = \frac{\dot{m}_s}{\rho_s (r_o - r_i) L} \Big/ \frac{\dot{m}_A}{\rho_A \pi r_i^2}$$

This quantity has been introduced and used in the past (e.g. Ref. (5)) to permit a direct comparison of the amount of swirl present in various experimental situations.

EXPERIMENTAL RESULTS

Before presenting details relating to the data acquired from this experimental investigation of co-axial, subsonic jet mixing in a supersonic stream, a consideration of the factors affecting the structure of the flow field is in order. A primary concern in the pretest procedure was the accuracy of centering the jet tube in the test section. Moreover, the symmetry of the problem and hence the repeatability of experiments hinged on this. By exercising extreme caution in the centering process, using a combination of template placement and wire adjustment, errors and non-uniformities resulting from jet off-centering were minimized. Another important factor was the interference effects of the wires. There were weak shocks due to the wires, and this meant a decrease in the test section Mach number. From measurements taken without the apparatus the Mach number was found to be 4.0 while from those taken with the apparatus the Mach number at the edge of the mixing region was found to vary between 3.1 and 3.6. At the points of attachment of the wires, there were also disturbances generated. These disruptions and the wires themselves introduced non-uniformities in the flow that slightly affect the measurements taken at stations in proximity of the jet exit. The exact character and the turbulent nature of the flow field is shown in the spark Schlieren photograph in Figure 8. It is evident that both the jet and the free stream were highly turbulent. The pipe Reynolds' number of the exiting jet was well above that required for turbulent pipe flow. The high

turbulence level in the free stream is produced by the support wires.

As indicated before, the experimental data consisted of pitot pressure, static pressure, and total temperature measurements. This data and the following calculated flow quantities are listed in Tables 1-7 in Appendix D: Mach number, total pressure, static temperature, velocity.

The total pressure distributions at the five axial stations that were examined are presented in Figure 9. In the first profile, X = 5D, it is seen that when port 7 was on the center line of the jet, a Gaussian like distribution was obtained. When P_c was on the center line, there was a decrease in total pressure in the vicinity of ports 5 and 6. This was due to the influence of the shock off the lip of the jet tube; port 5 was located essentially at the position of the shock. Since the remaining ports were in front of the shock, there was an obvious increase in total pressure in order to satisfy the external flow conditions. At X = 10D, 15D, 20D, normal Gaussian error curves were obtained from the pressure surveys. As for X = 25D, the total pressure also varied in a Gaussian fashion when port 7 was at the center of the jet. However, ports 3-0 with P_c on the center line showed a small decrease in total pressure. This pressure change is attributed to non-uniformities in the external flow field.

In Figure 10 the Mach number profiles are given. An inspection of stations 5D-25D revealed the same basic trend indicated by the corresponding total pressure distributions. However, it should be noted that when the rake was centered at 5D, ports 10 through 4 were in the inviscid core

of the jet, and these Mach numbers were necessarily subsonic. Consequently, the 10° half-angle cone static probe could not be used to determine static pressure in this region. Despite the lack of experimental support for this station, it was considered reasonable to take the static pressure as constant across the mixing layer. At the other stations, the maximum percentage change in static pressure across the jet was found to be 8%. All Mach numbers were therefore calculated on the basis of constant static pressure across the layer. These Mach numbers were used to obtain the static temperature variations as mentioned previously.

The velocity profiles, derived from the static temperature and Mach number distributions, are shown in Figure 11. In Figure 13, a log-log graph of the non-dimensionalized velocity deficit,

$$\frac{U_E(x)-U_C(x)}{U_E(x)}$$

versus X/D is given. A plot of the velocity defect decay of this type assumes the same general form over a wide range of flow conditions and configurations, i.e. wake and jets at low and high speeds. For large X/D, the curve becomes a straight line indicating that the defect decays as $(X/D)^{-n}$. For the case under discussion here n = -.828.

The Schlieren photographs in Figures 7a and 7b show the shock coming from the lip of the jet tube. This was the strongest shock in the flow field. The shocks off the wires can also be seen. A careful examination of these photographs disclosed that there were no perceptible gross effects of the swirl. In addition, a comparison of the total pressure profiles for the swirl case, given in Figure 12, and the non-swirl case also showed no discernible effect of the swirl in aiding the mixing.

The swirl number, a measure of the degree of swirl, was 1.97. To verify that swirl was being produced by the tangential injection, no swirl and swirl tests were run with Helium as an injectant and no external stream. Schlieren photographs were taken and compared. These showed a significant increase in the spread angle of the jet for the swirl case. Therefore, the production of swirl by the system was established. However, since the ratio of the diameter of the holes in the swirl tube to the diameter of the tube itself was .545, it was felt that the system was possibly not producing the maximum degree of swirl possible. Consequently, a complementary set of tests at X = 10D were performed with a slightly modified set-up. That is, flow baffles were soldered in front of each hole in order to make sure that the flow entered perpendicular to the axial flow, and therefore, a high degree of swirl was being achieved. Both the Schlieren photographs and the pitot pressure data taken indicated no appreciable effect of the swirl.

DISCUSSION

These tests of co-axial jet mixing at a high free stream Mach number show the flow field to resemble that of the wake behind a high speed body more than that previously observed for jets at low Mach numbers. The presence of a lip shock closely adjacent to the viscous region and the very slow axial growth of mixing region width leave only the characteristic near-wake separation bubble absent.

The data provide a stringent test against which turbulent mixing analyses can be refined. Of particular interest, is the result that initial swirl offers little promise as a mixing aid when the external stream is at very high speeds. It is simply not practical to produce swirling velocities that are large compared to the axial components of the free stream when that is supersonic.

REFERENCES

1. Abramovich, G. N., The Theory of Turbulent Jets, MIT Press, Cambridge (1963).

2. Schetz, J. A., "Unified Analysis of Turbulent Jet Mixing", NASA CR-1382 (1969).

3. Schetz, J. A., "Some Studies of the Turbulent Wake Problem", Astronautica Acta (1971).

4. Chigier, N. A. and Chervinsky, A., "Experimental Investigation of Swirling Vortex Motion in Jets", Journal of Applied Mechanics (1967).

5. Swithenbank, J., and Chigier, N. A., "Vortex Mixing For Supersonic Combustion; Portier, France (1968).

6. Sims, J. L., Tables For Supersonic Flow Around Right Circular Cones At Zero Angle Of Attack, NASA SP-3004 (1964).

7. Equations, Tables, And Charts For Compressible Flow, NACA Report 1135 (1953).

8. Handbook of Supersonic Aerodynamics. Section 20, Wind Tunnel Instrumentation and Operation, Bureau of Naval Weapons Publication (1961).

APPENDIX A

(ERROR ANALYSIS)

APPENDIX A

The following information concerns the calculation of the maximum possible error in the measured and computed data. A table of the experimental errors is given at the end of the discussion.

Pitot and Cone Static Pressures.--It is estimated that the measured pitot and cone static pressures are within ±2% of their actual values. This percentage is based primarily on error occurring in the following: 1) calibration of the transducer; 2) reading from the strip chart recorders; 3) reading from the calibration curve.

Mach number.--In order to determine the maximum error in Mach number, the ratio of the maximum static pressure to the minimum pitot pressure and the ratio of the minimum static pressure to the maximum pitot pressure are found. A close examination of the data taken at each station, both the no swirl and swirl cases, revealed that the 15D station on the center line would adequately reflect the maximum error in static pressure. Using a plus sign for maximum and a minus sign for minimum, we have

$$\frac{p_1^+}{p_{t_2}^+} \rightarrow M = 1.84$$

$$\frac{p_1^-}{p_{t_2}^+} \rightarrow M = 1.97$$

Since the measured Mach number is 1.93, the variation in Mach number is +3.14%, -3.66%.

Total Pressure, Static Temperature, Velocity.--Still using station 15D as a base, the errors in total pressure, static temperature and velocity are computed.

TABLE A-1

ESTIMATE OF ERRORS IN MEASURED
AND CALCULATED QUANTITIES

Quantity	Estimated Error - %
Pitot pressure	±2.0
Static pressure	+4.1 -3.7
Mach number	+3.14 -3.66
Total pressure	±5.86
Static temperature	+1.90 -3.79
Velocity	+4.15 -5.53

APPENDIX B

(SUPERSONIC WIND TUNNEL)

APPENDIX B

9" x 9" SUPERSONIC WIND TUNNEL

The V.P.I. 9 x 9 in. supersonic wind tunnel was designed and originally constructed at the Langley Aeronautical Laboratory. In 1958 the tunnel was purchased by V.P.I. and after being re-constructed in a specially designed building was put into operation in 1963. During recent years several modifications were introduced into the air pumping, tunnel control and instrumentational equipment which increased capabilities of the facility.

The facility is of an intermittent, blow-down type with interchangeable contoured nozzles. The air pumping system consists of eight Ingersoll Rand, Model 90, reciprocating compressors, of 800 hp total capacity. They can pump the storage system up to 150 psig. A very efficient drying and filtering system is provided which includes both drying by cooling and drying by adsorption. The latter is accomplished by a fully automated system fabricated by the Kamp Co. and uses molecular sieves and activated alumina as desiccant. Air storage system consists of 16 tanks with a total volume of 2800 $ft.^3$. Tunnel control system includes a quick opening butterfly valve and a pressure regulating system.

The settling chamber contains a perforated transition cone, several damping screens and probes measuring stagnation pressure and temperature. The nozzle chamber is interchangeable with two-dimensional contoured nozzle blocks made of steel. The tunnel is equipped with three complete nozzle

chambers which presently are fitted with the nozzles for the Mach numbers 2.4, 3, and 4. Several other nozzle blocks are available (not calibrated).

The working section of the tunnel is equipped with a remotely controlled model support which allows one to vary the position of a model in the vertical plane.

An arrangement for side wall model mounting is also available. An extractable mechanism can be provided for supporting the model during the starting and stopping of the flow. Due to large windows in the nozzle and working sections a very good access to the model is ensured.

After passing through a diffuser the air flow is discharged into the atmosphere outside of the building.

Technical Specification of the tunnel:

Test Section size	9 x 9 inches
Stagnation pressure	40 - 120 psia
Mach number	2.4 - 4
Reynolds number per foot	6×10^6 to 15×10^6
Run duration, depending on	
Mach number	10 - 90 sec.
Dewpoint	below -40°C
Maximum model diameter at M=3	3.5 in.
Storage tank volume	2800 $ft.^3$
Maximum air pressure in	
the storage tanks	150 psig
Total power rate of the	
compressor plant	800 hp

APPENDIX C

(MASS FLOW METERS)

APPENDIX C

The capacity of flow meter FM1 was found to be 3.24 scfm at standard temperature and pressure. For any other operating pressure, denoted by P_{op}, the maximum mass flow was calculated from

$$3.24 \sqrt{\frac{P_{op}}{14.7}}$$

For example, in the no swirl tests performed the capacity of FM1 was

$$3.24 \sqrt{\frac{19.4+13.7}{14.7}} = 4.87 \text{ scfm},$$

which corresponded to a reading of .800 on the meter. As stated previously, the desired setting was determined experimentally. The reading was .225 which meant a mass flow of

$$\frac{.225}{.800} (4.87) = 1.37 \text{ scfm} .$$

In the swirl case where

$$P_{op} = \frac{33.1}{2} = 16.55 \text{ psia} \rightarrow 2.9 \text{ psig}$$

was chosen for FM1, the full scale mass flow was 3.44 scfm. Since it was desired to have 50% of the injected air in the axial direction, the meter was set at

$$\frac{.685}{3.44}\ (.800) = .16 \text{ scfm.}$$

The operating conditions prescribed on FM2 were 30 scfm of CO_2 at 30 psig and 80°F. In order to convert to scfm of air at standard conditions, the following formula was used:

$$\begin{matrix}\text{scfm of air} \\ @\ 14.7\ \text{psia} \\ \text{and } 70°\text{F}\end{matrix} = \begin{pmatrix}\text{scfm of} \\ \text{gas}\end{pmatrix}\left[\frac{\text{sp. gr } (14.7)\left(T_{op}\right)(8.02)}{1.0\ (P_{op})(530)(\rho_f)}\right]^{1/2},$$

where T_{op} is absolute operating temperature and ρ_f is the density of the float. Therefore,

$$\begin{matrix}\text{scfm of air} \\ @\ 14.7\ \text{psia} \\ \text{and } 70°\text{F}\end{matrix} = \left(\frac{30}{60}\right)\left[\frac{1.52(14.7)(540)(8.02)}{1.0(44.7)(530)(8.02)}\right]^{1/2}$$

$$= \frac{\sqrt{.509}}{2}$$

$$= .357$$

With P_{op} = 153.7 psia in the swirl tests, the full scale setting of 30 meant

$$.357\ \sqrt{10.46} = 1.15 \text{ scfm .}$$

Since half of the mass flow was injected tangentially, the mass flow setting for FM2 was

$$\frac{.685}{1.15} (30) = 17.87 \text{ scfm} .$$

APPENDIX D

(TABULARIZED EXPERIMENTAL DATA)

TABLE D-1

STATION 5D

	P_c = 2.61 psia		P = 1.61 psia		
PORT	P_{t_2} (psia)	M	P_{t_1} (psia)	T(°R)	U(FPSx10^{-2})
8	1.99	.56	1.99	508	6.19
7	1.97	.55	1.97	509	6.08
10	1.80	.41	1.80	522	4.59
9	1.84	.45	1.84	519	5.02
5	1.95	.53	1.95	511	5.87
4	2.84	.94	2.84	459	9.87
3	5.04	1.43	5.30	383	13.72
2	10.48	2.17	16.33	278	17.74
1	15.77	2.69	36.92	221	19.61
0	22.20	3.21	81.08	176	20.90
8*	19.73	3.04	62.20	190	20.51
7*	20.50	3.09	67.47	186	20.63
10*	19.18	2.92	54.54	200	20.22
9*	20.85	3.13	71.04	182	20.72
5*	19.83	3.04	62.52	190	20.51
4*	20.66	3.11	69.19	184	20.68
3*	21.09	3.13	71.86	182	20.72
2*	20.97	3.12	70.84	183	20.70
1*	20.74	3.11	69.46	184	20.68
0*	20.50	3.09	67.48	186	20.63

*P_c on center line.

TABLE D-2

STATION 10D

	P_c = 2.30 psia		P = 1.41 psia		
PORT	P_{t_2} (psia)	M	P_{t_1} (psia)	T(°R)	U(FPSx10^{-2})
8	6.07	1.72	7.16	339	15.53
7	4.89	1.52	5.30	369	14.32
10	6.71	1.82	8.35	325	16.08
9	6.71	1.82	8.35	325	16.08
5	5.89	1.69	6.85	344	15.35
4	6.84	1.84	8.61	322	16.18
3	8.00	2.02	11.24	297	17.07
2	10.30	2.31	17.79	261	18.30
1	13.94	2.71	33.18	219	19.64
0	19.88	3.26	75.82	173	21.00
8*	18.77	3.16	65.63	180	20.79
7*	21.84	3.41	94.87	162	21.30
10*	22.56	3.47	103.20	158	21.41
9*	19.08	3.20	69.08	177	20.88
5*	22.09	3.44	98.48	160	21.35
4*	22.51	3.46	102.09	159	21.39
3*	22.74	3.49	105.87	157	21.44
2*	22.78	3.50	107.00	157	21.46
1*	22.78	3.50	107.00	157	21.46
0*	22.75	3.49	105.91	157	21.39

*P_c on center line.

TABLE D-3

STATION 15D

	P_c = 1.93 psia		P = 1.18 psia		
PORT	P_{t_2} (psia)	M	P_{t_1} (psia)	T(°R)	U(FPSx10^{-2})
8	6.89	2.04	9.81	295	17.16
7	6.12	1.91	8.02	312	16.54
10	6.86	2.04	9.77	295	17.16
9	6.42	1.96	8.68	305	16.79
5	6.75	2.02	9.49	297	17.07
4	7.31	2.11	10.92	286	17.48
3	8.19	2.25	13.53	268	18.06
2	9.86	2.47	19.29	243	18.88
1	12.71	2.83	33.47	208	19.98
0	16.79	3.22	61.84	176	20.92
8*	14.19	3.00	43.22	193	20.42
7*	17.36	3.22	63.94	176	20.92
10*	17.81	3.36	74.09	166	21.20
9*	15.17	3.11	50.80	184	20.68
5*	19.42	3.52	92.79	155	21.50
4*	19.95	3.57	99.55	152	21.58
3*	20.28	3.60	103.84	150	21.63
2*	20.65	3.64	110.02	148	21.70
1*	20.91	3.65	111.76	147	21.72
0*	21.02	3.66	113.32	147	21.73

*P_c on center line.

TABLE D-4

STATION 20D

	P_c = 1.78 psia		P = 1.13 psia		
PORT	P_{t_2} (psia)	M	P_{t_1} (psia)	T(°R)	U(FPSx10^{-2})
8	7.43	2.18	10.26	277	17.78
7	6.92	2.10	11.66	287	17.43
10	7.65	2.22	12.36	272	17.94
9	7.71	2.22	12.45	272	17.94
5	7.52	2.19	11.89	276	17.82
4	7.93	2.26	13.19	267	18.10
3	8.41	2.33	14.75	259	18.37
2	9.32	2.46	18.09	244	18.84
1	11.14	2.70	26.30	220	19.61
0	14.45	3.10	47.97	185	20.65
8*	12.54	2.88	34.46	203	20.12
7*	14.93	3.15	51.75	181	20.77
10*	15.92	3.25	60.19	174	20.98
9*	15.02	3.16	52.52	180	20.79
5*	16.91	3.35	69.73	166	21.18
4*	17.35	3.40	74.72	163	21.28
3*	17.63	3.43	77.91	161	21.33
2*	17.79	3.44	79.31	160	21.35
1*	18.05	3.47	85.57	158	21.41
0*	18.52	3.51	87.73	156	21.48

*P_c on center line.

TABLE D-5

STATION 25D

	P_c = 2.00 psia		P = 1.25 psia		
PORT	P_{t_2} (psia)	M	P_{t_1} (psia)	T(°R)	U(FPSx10^{-2})
8	8.81	2.26	14.66	267	18.10
7	8.37	2.20	13.33	274	17.86
10	8.90	2.27	14.92	266	18.14
9	8.96	2.27	15.02	266	18.14
5	8.86	2.26	14.74	267	18.10
4	9.24	2.31	15.84	261	18.30
3	9.76	2.38	17.79	253	18.56
2	10.72	2.50	21.48	240	18.98
1	12.56	2.72	30.15	218	19.67
0	16.11	3.11	53.95	184	20.68
8*	14.31	2.92	40.68	200	20.22
7*	17.05	3.19	61.20	178	20.85
10*	18.12	3.29	70.92	171	21.06
9*	16.96	3.19	60.87	178	20.85
5*	19.03	3.38	80.53	164	21.24
4*	19.39	3.40	83.50	163	21.28
3*	19.08	3.38	80.74	164	21.24
2*	18.50	3.32	74.32	169	21.12
1*	18.66	3.34	76.29	167	21.16
0*	18.64	3.33	75.53	168	21.14

*P_c on center line.

TABLE D-6

TOTAL PRESSURE PROFILES[†]
(SWIRL)

PORT	5 D	10 D	15 D	20 D	25 D
8	2.06	8.03	10.32	12.49	15.34
7	1.74	5.54	7.33	10.54	14.16
10	1.71	6.21	9.03	12.71	15.85
9	1.72	7.00	8.13	12.52	15.83
5	2.03	7.47	9.10	12.12	15.85
4	2.73	9.47	10.74	13.13	17.21
3	4.72	12.66	13.04	14.71	19.16
2	14.92	19.02	18.66	18.04	23.73
1	34.80	35.77	31.99	26.56	34.00
0	74.99	78.89	62.92	48.17	60.96
8*	60.72	63.75	41.35	33.19	43.10
7*	71.72	94.49	67.50	50.63	68.22
10*	65.87	101.21	78.47	59.44	73.63
9*	70.86	67.41	50.54	51.99	64.23
5*	64.67	93.98	92.64	69.30	84.71
4*	69.80	100.00	99.25	74.00	87.94
3*	73.46	103.31	104.86	76.14	86.20
2*	73.15	103.13	108.09	79.49	78.82
1*	70.66	103.13	112.78	81.34	80.32
0*	68.38	103.36	115.36	87.82	80.49

[†]Pressures in psia.

TABLE D-7

$\frac{X}{D}$	$\frac{U_E(X)-U_C(X)}{U_E(X)}$
5	.7158
10	.3305
15	.2388
20	.1885
25	.1552

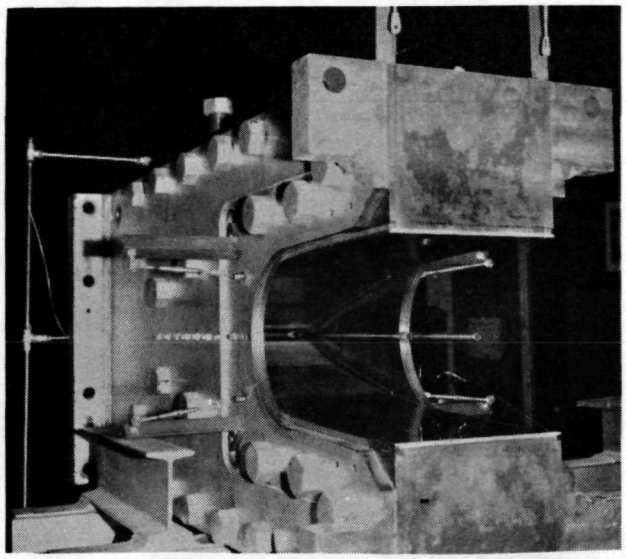

(a)

1 OF 2
AXIAL FLOW
ENTRANCES

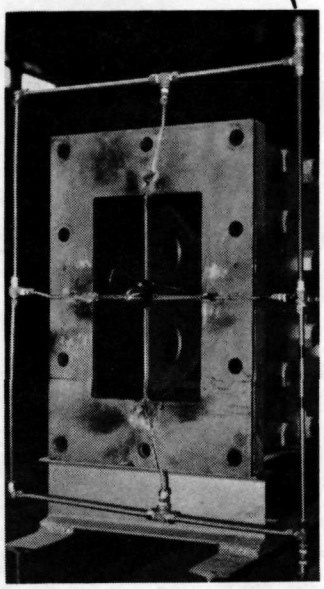

(b)

RAKE

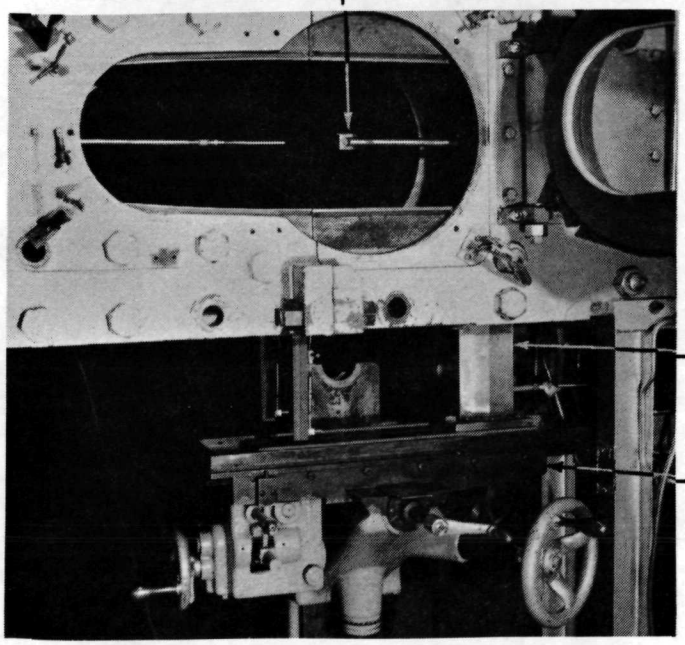

STRUT

MILL BED

(c)

FIG. 1 EQUIPMENT

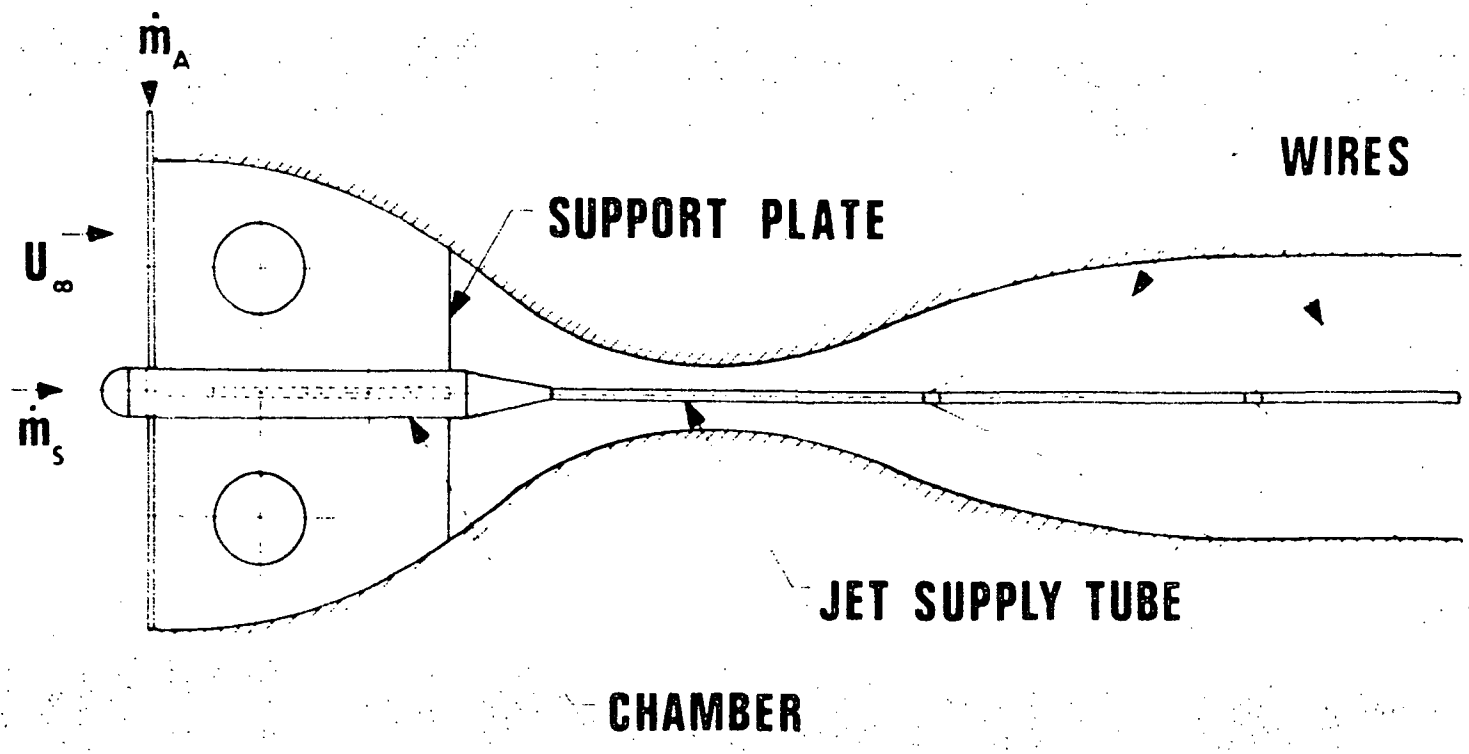

FIG. 2 APPARATUS DETAILS

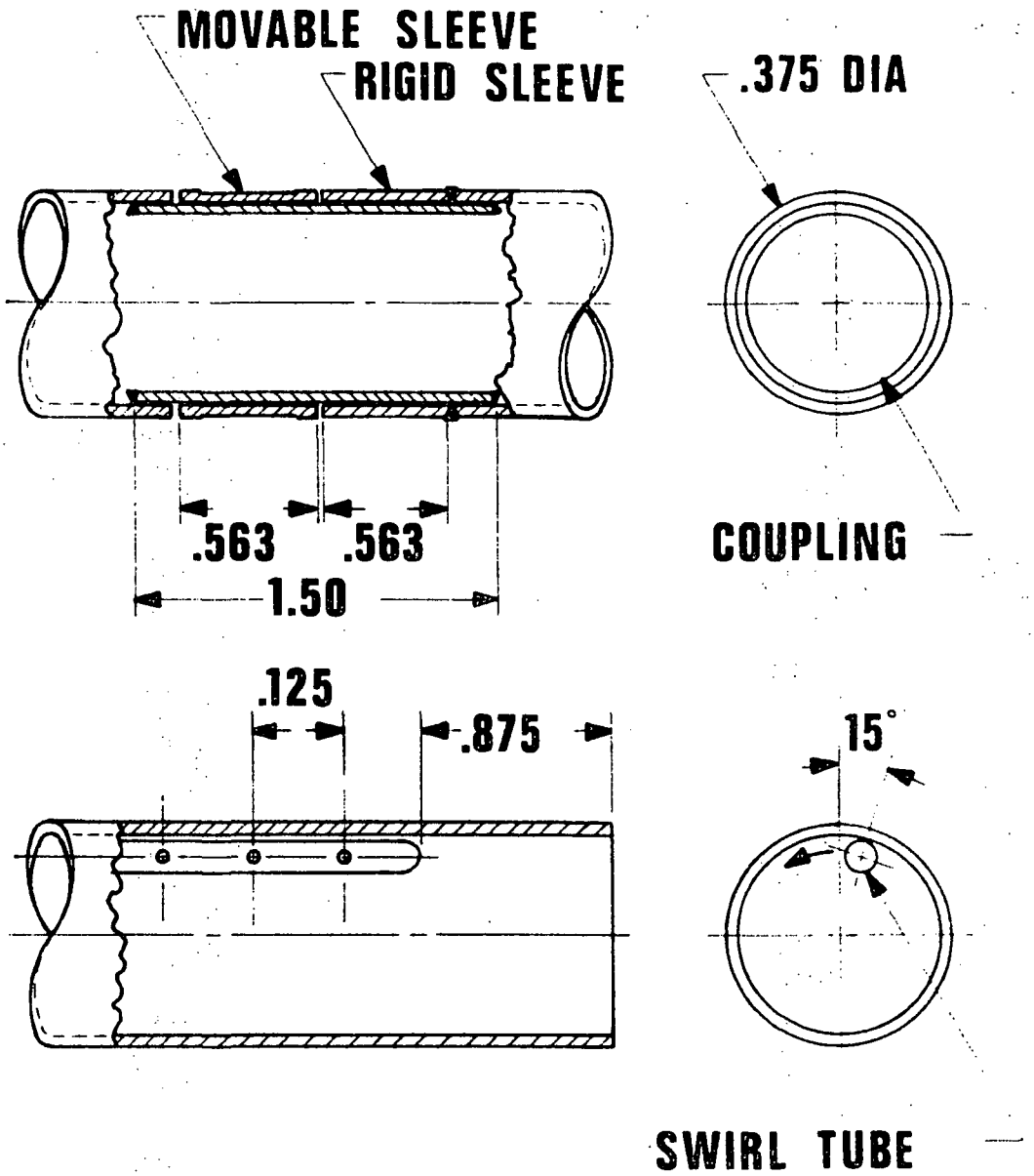

FIG. 3 JET SUPPLY TUBE DETAILS

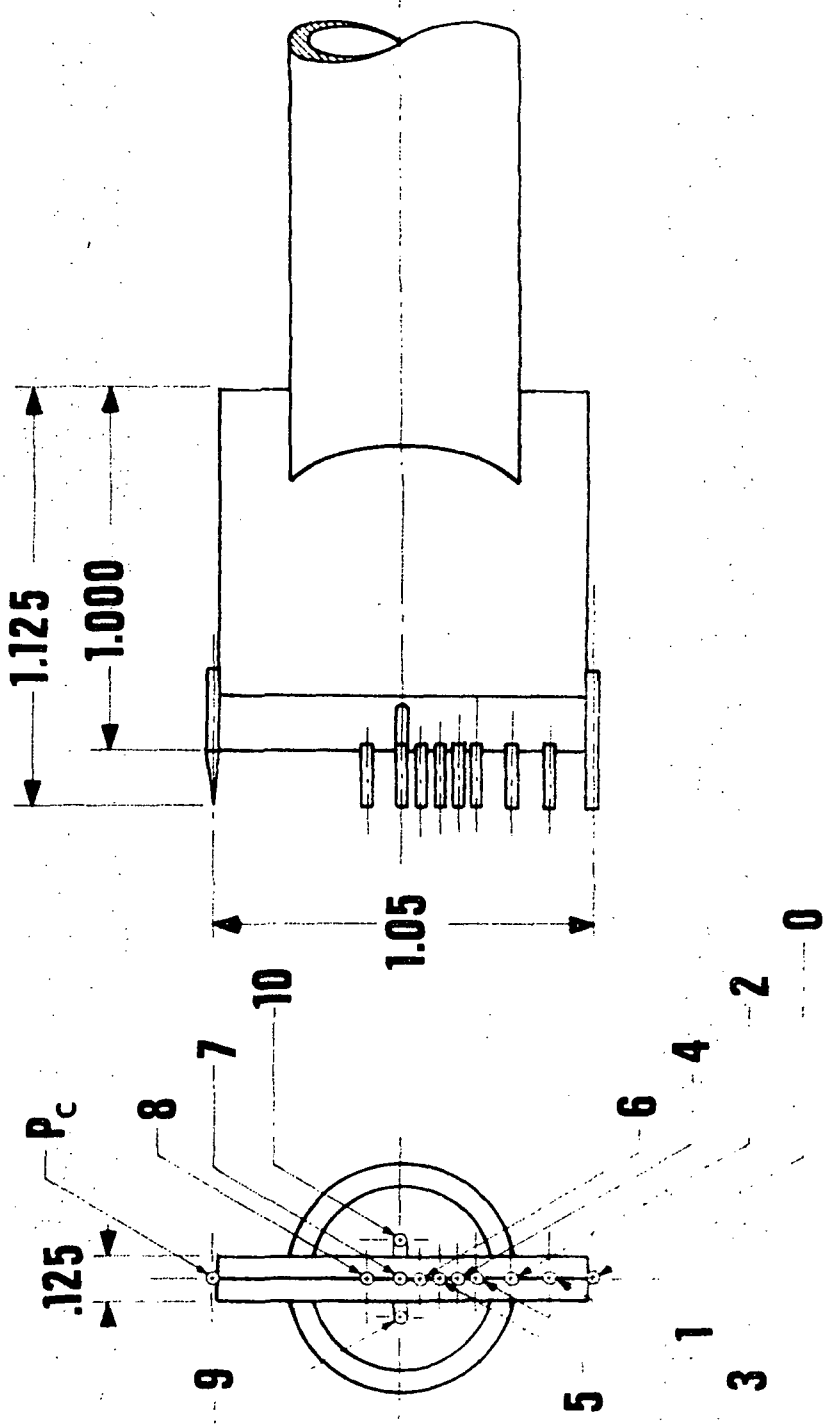

FIG. 4 RAKE DETAILS

TABLE D-8

PRESSURE RAKE

Port Numbers	Distances (in.)
P_c-7	.524
8-7	.100
9-7	.100
10-7	.100
7-6	.050
6-5	.050
5-4	.050
4-3	.050
3-2	.100
2-1	.100
1-0	.125

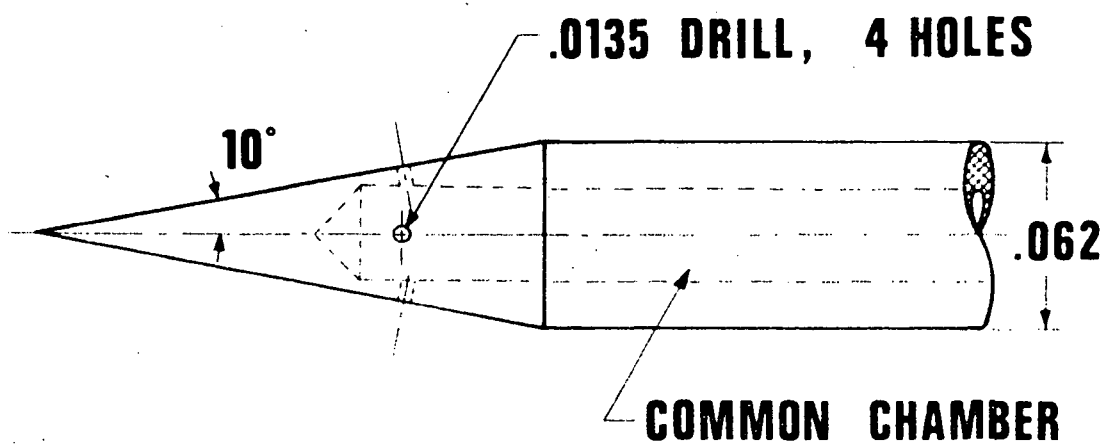

FIG. 5 CONE STATIC PROBE

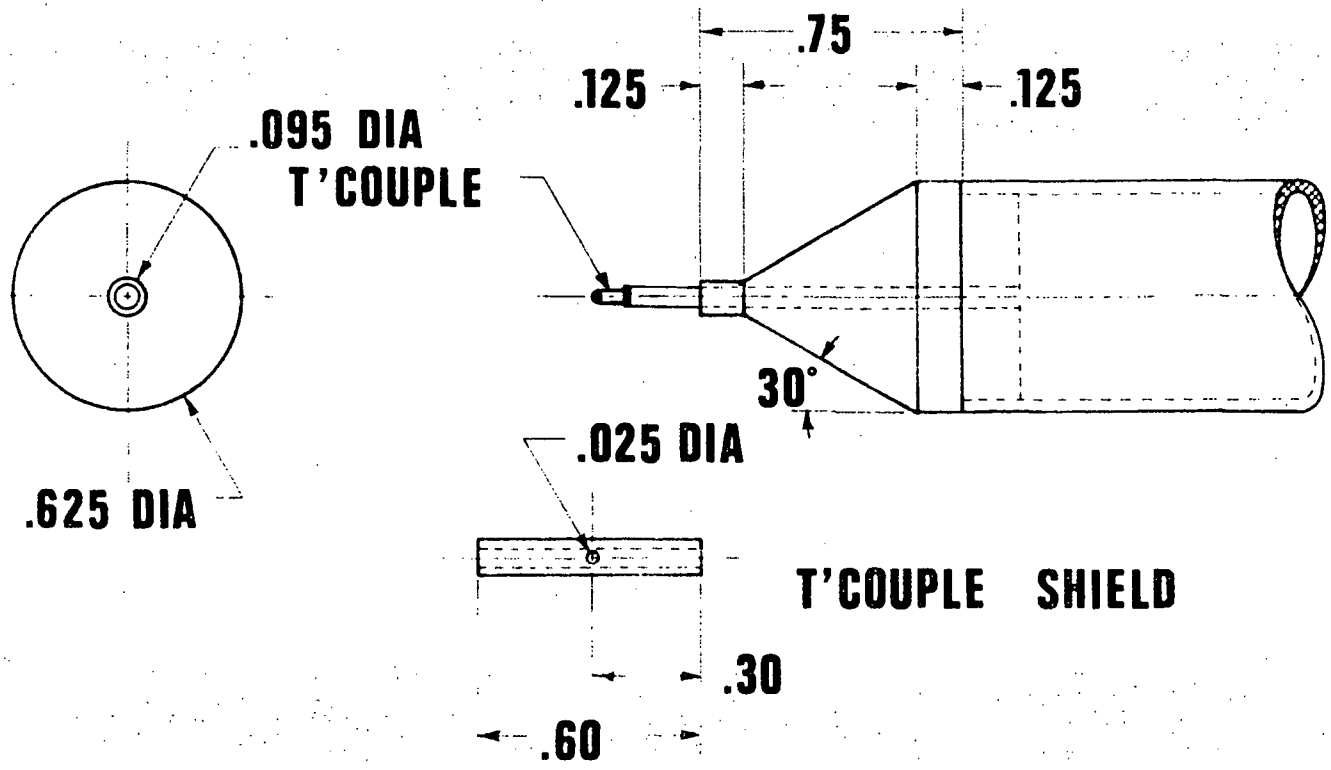

FIG. 6 TEMPERATURE PROBE

(a)

NO SWIRL

(b)

SWIRL

FIG. 7 SCHLIEREN PHOTOGRAPHS (X=10D)

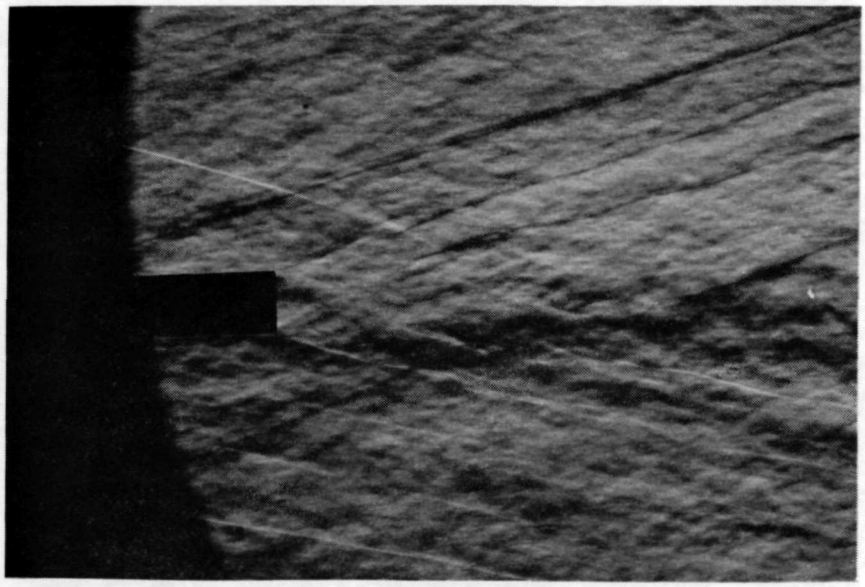

FIG. 8 SPARK SCHLIEREN PHOTOGRAPH

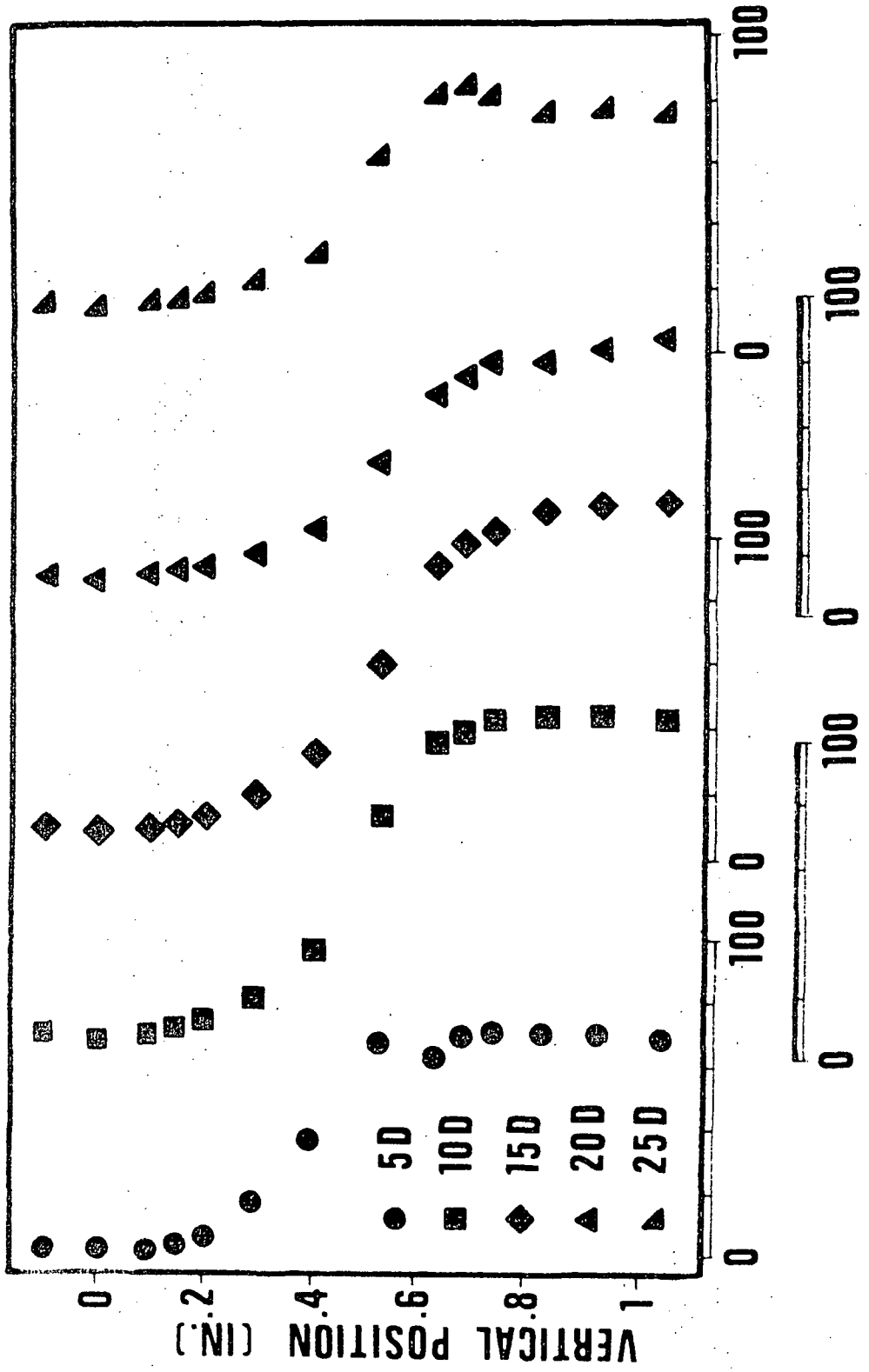

FIG. 9 TOTAL PRESSURE PROFILES

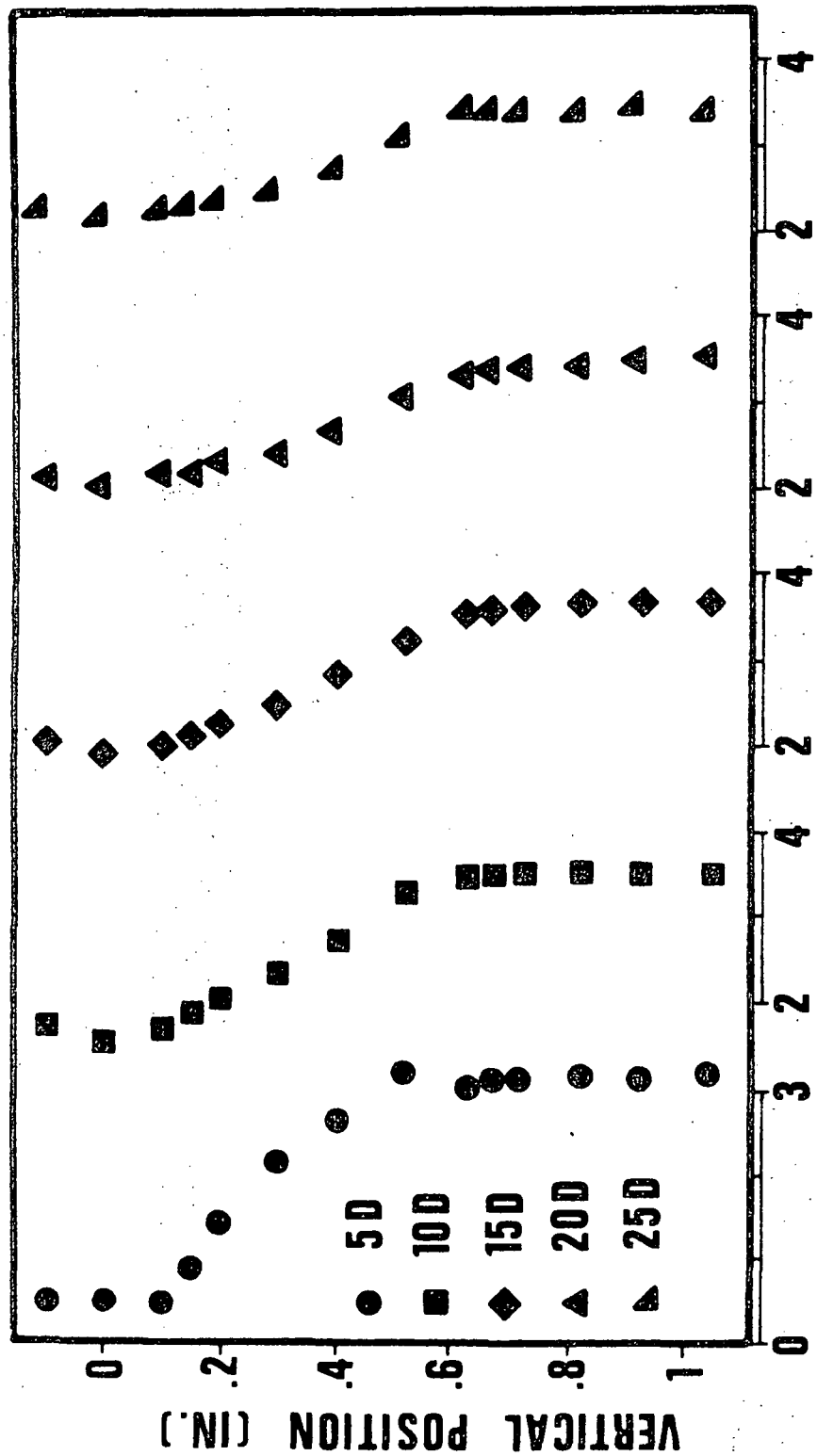

FIG. 10 MACH NUMBER PROFILES

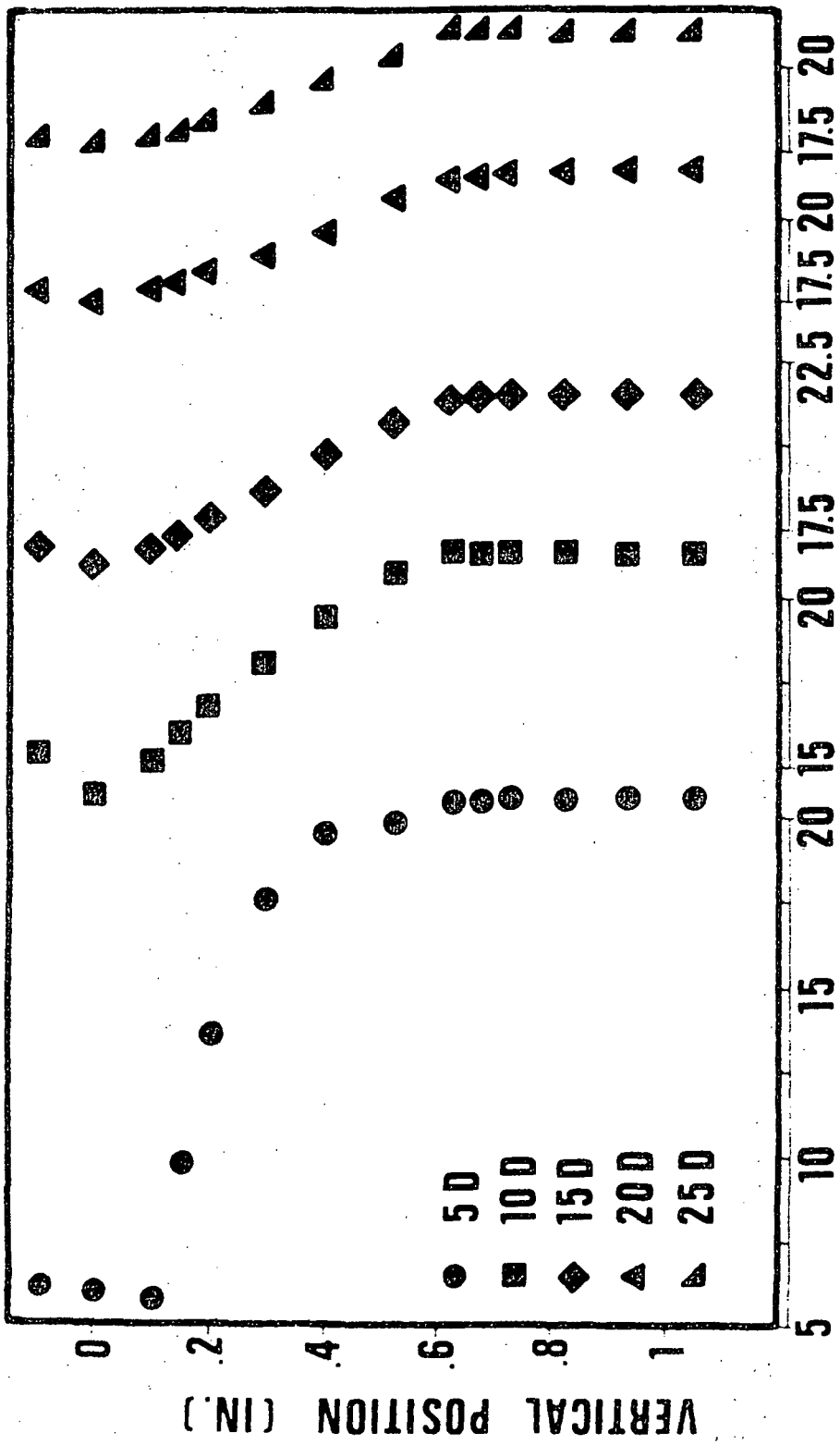

FIG. 11 VELOCITY PROFILES

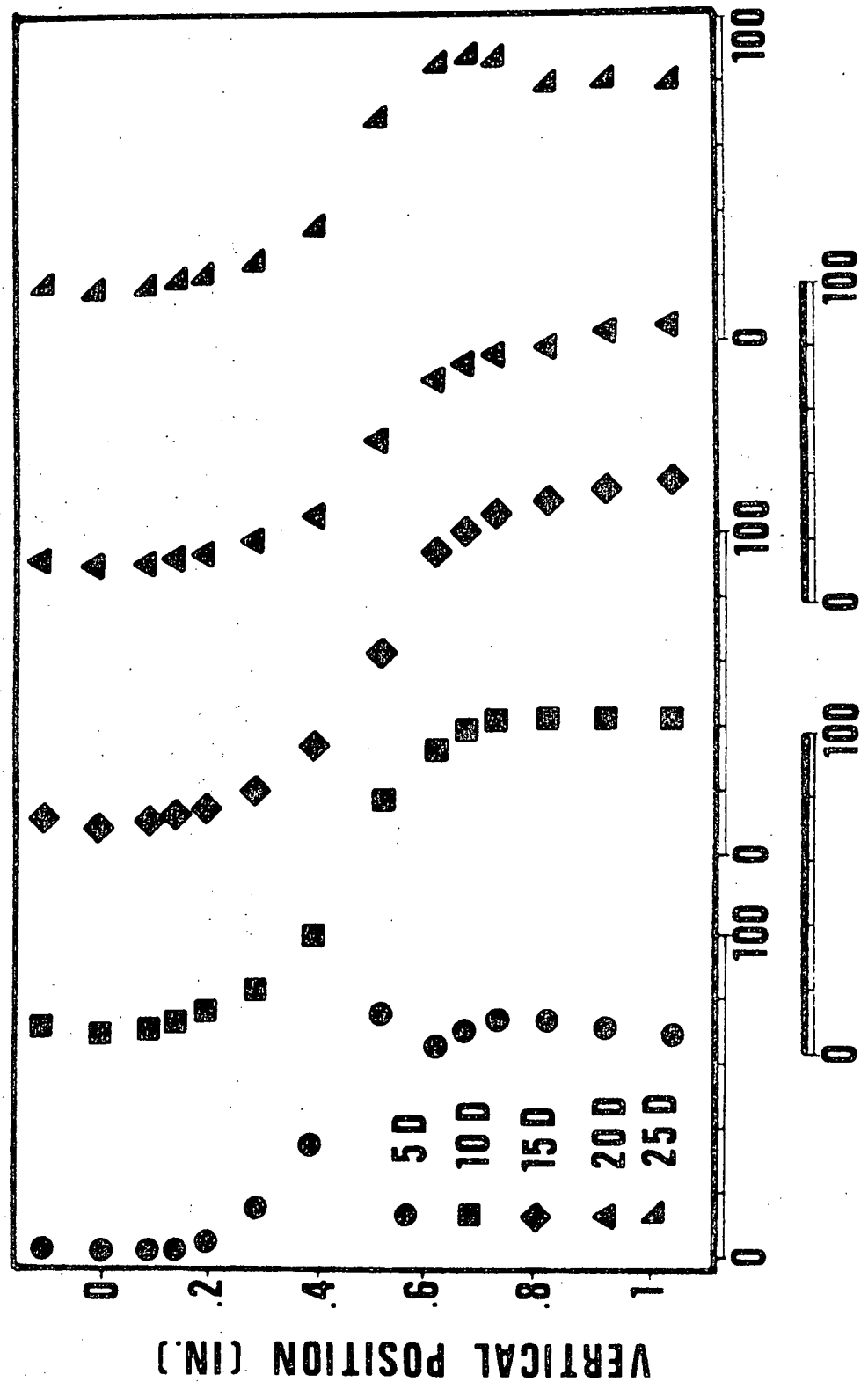

FIG. 12 TOTAL PRESSURE PROFILES (SWIRL)

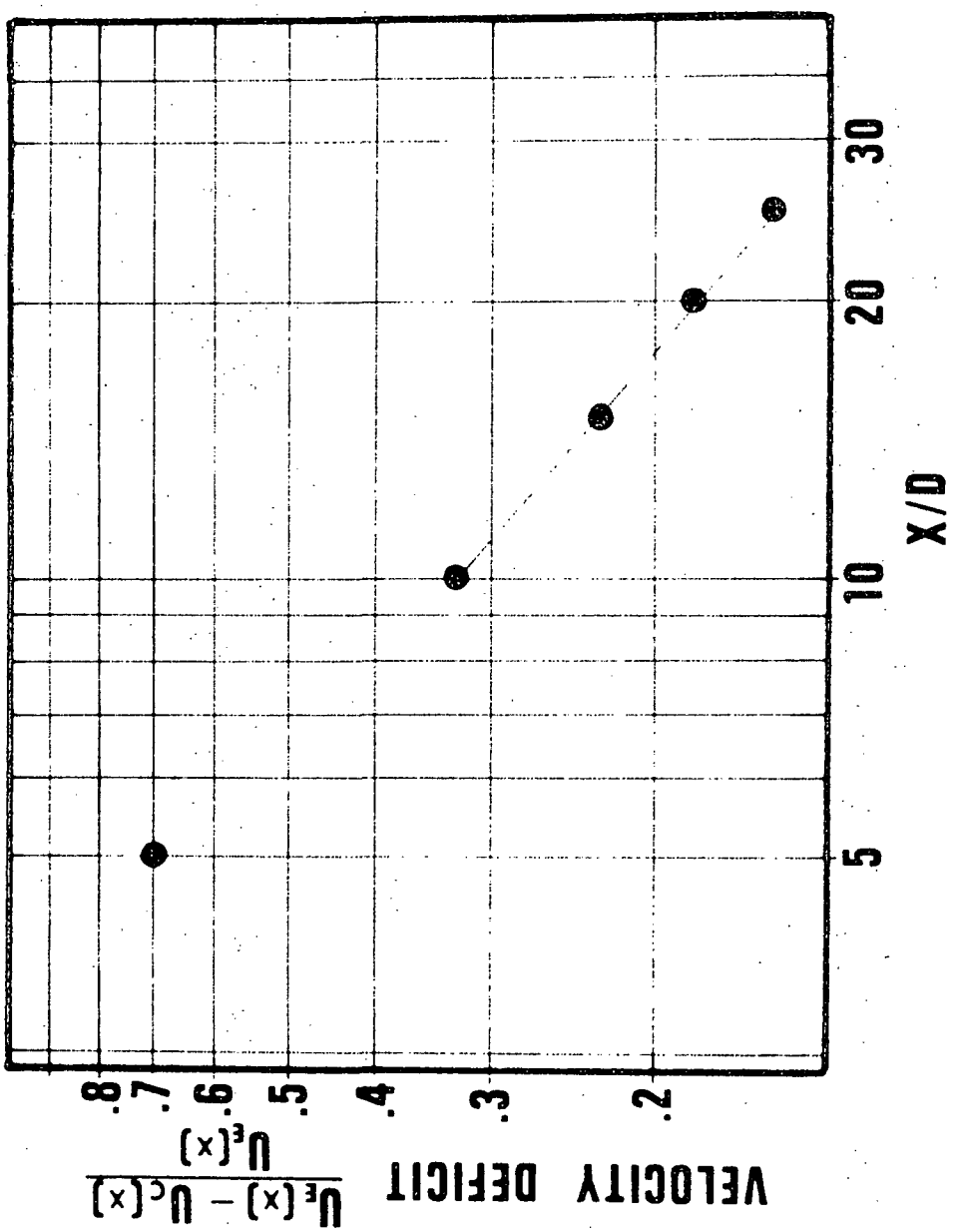

FIG. 13 VELOCITY DEFICIT VS. X/D